Investigating the Influences of Two Position (Non-Staggered and Staggered) of Wind Turbine Arrays to produce power in a Wind Farm

by Ismail Ismail

Investigating the Influences of Two Position (Non-Staggered and Staggered) of Wind Turbine Arrays to produce power in a Wind Farm

Ismail$^{1, 4, a)}$, Samsul Kamal^2, Purnomo^2, and Sarjiya^3

[1]*Mechanical Engineering Postgraduate Student, Department of Mechanical and Industrial Engineering, Universitas Gadjah Mada, Jl. Grafika No. 2, Yogyakarta 55281, Indonesia*
[2]*Mechanical Engineering, Department of Mechanical and Industrial Engineering, Universitas Gadjah Mada, Jl.Grafika No. 2, Yogyakarta 55281, Indonesia*
[3]*Electrical Engineering, Department of Electrical and Information Engineering Universitas Gadjah Mada, Jl.Grafika No. 2, Yogyakarta 55281, Indonesia*
[4]*Mechanical Engineering, Department of Mechanical Engineering, Universitas Pancasila, Jl. Srengseng Sawah, Jagakarsa, Jakarta, Indonesia*

a)Corresponding author: ismail2k7@gmail.com

Abstract. This investigation was conducted to identify the influences of the two positions (non-staggered and staggered) of wind turbine arrays. Identification on down-scaled size wind turbine arrays was carried out in an open circuit, suction-type wind tunnel. Based on the results of the experiment, empirical relations for the centreline velocity deficit, tipline velocity deficit and wake radius are proposed. The non-staggered position results are larger power generated than that of the staggered position, this influenced by the trend deficit in velocity that makes wind turbine generated power difference between staggered position and non-stagger position. The area used non-staggered position larger than staggered position. Result staggered position has become one of the solutions to harness wind farms confined areas.

Keyword: Non-staggered position, staggered position, wind tunnel, wakes flow.

INTRODUCTION

Understanding and quantifying the effect of natural and wind turbine on turbulent flows is essential to propose or validate new turbulence closure schemes and to provide a simplified representation of complex boundary conditions necessary for improved predictive modelling [1-11]. The layout and array of a wind turbine in the wind farm depend on a detailed knowledge of the development of the wake flow of a wind turbine. It is important to understand the interaction between the wake flow of a wind turbine and the atmospheric turbulence in order to predict its structural load and power performance [12, 13]. Most studies divided the wake effect into the near wake and far wake regions [14, 15]. The near wake region is considered to extend downwind of the rotor up to 1-3 rotor diameters. The far wake region [16, 17] has found that the velocity distribution in the turbine wake exhibits a self-similar behaviour. This region is characterized by the blade aerodynamics and the evolution of tip vortices [18].
The velocity deficit U_{c0} (=U_0-U_c) at the centerline of the turbine wake can be described by the following equation:

$$\frac{U_{c0}}{U_0} = k\left(\frac{r}{z}\right)^n \tag{1}$$

Proceedings of the 3rd AUN/SEED-NET Regional Conference on Energy Engineering and the 7th International Conference on Thermofluids (RCEnE/THERMOFLUID 2015)
AIP Conf. Proc. 1737, 040006-1–040006-10; doi: 10.1063/1.4949294
Published by AIP Publishing. 978-0-7354-1391-7/$30.00

Where U_0 is undisturbed wind velocity at the hub height, U_c is the time averaged velocity at the centerline of wake flow, r is the rotor radius, z is the downwind distance from the turbine, and k & n are constants. The experimental results show that these constants are in the range $1 < k < 3$, and $0.75 < n < 1.25$ [5, 3].

Numerical results from Ismail *et al* [19] show that rectangular horizontal wind farm design with a rotor diameter 113 m, for spacing wind turbines in rows apart in the windward direction 1.77 rotor diameters and apart in the crosswind direction 8.85 rotor diameters constitutes of the most optimal result. The wind tunnel is used to investigate the influence of wake effect and power production in this study. Wind turbines and area are used in this study to represent a wind farm to a down-scale condition of the full-scale. Studies investigating the influence of positions both staggered and non-staggered position is done to show the trend of wind speed in the two positions and the power generated. This result can be a consideration in the determination of the position of wind turbine arrays used.

EXPERIMENTAL SET UP

The experiments were carried out in an open-circuit, suction-type wind tunnel. The wind tunnel used belongs to the laboratory of heat transfer & mass and mechanics fluid, Department of Mechanical Engineering, Universitas Gadjah Mada. This wind tunnel has an overall dimension with the length of 7.59 m, wide 1.84 m and high 1.88 m, and also provided with the transparent wall and top at test section. Special on test section has the dimensions of long 2.44 m, wide 1.84 m and high 0.45 m.Testing the model wind farms is done by using the principle of similarity. The similarity in this study is the similarity dimension to scale down. Tests on the study were conducted using area models and models of wind turbines, the principle of modelling is reshaping the existing problems in the prototype with comparable figures, so that in the event that the model is congruent with the conditions in the prototype.

The rotor blades of the wind turbine model used for the present study are made by machine 3-D Printing Fortus 250 MC with material ABS-M30. Airfoil used is NACA 4421. The blade dimension is from at root position to at tip as shown in Figure 1. A small electricity generator was installed in the back of the turbine blades, which would produce electricity as driven by the rotating turbine blades.

Chord (mm)	Twist (degree)
12.5	1.71
13.24	2.84
14.25	4.71
15.34	6.93
16.4	9.62
17.52	12.88
18.29	16.86
19.32	21.71
16.81	27.5
12	34.28

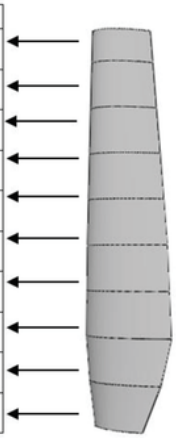

FIGURE 1. The blade dimension from at root position to at tip

The wind turbine model used for the present study represents the most widely-used three-blade horizontal axial wind turbine (HAWT) in wind farm of scale smaller than it really is. As shown in Figure 2, the rotor diameter of the wind turbine model was 0.2 m, the height of the turbine hub is 0.177 m above the wind tunnel floor, and the diameter of the turbine tower (circular pole) is 0.01 m. With the scale ratio of 1: 565, the test model would represent a wind turbine in a wind farm with the rotor diameter about 113 m and tower height about 100 m.

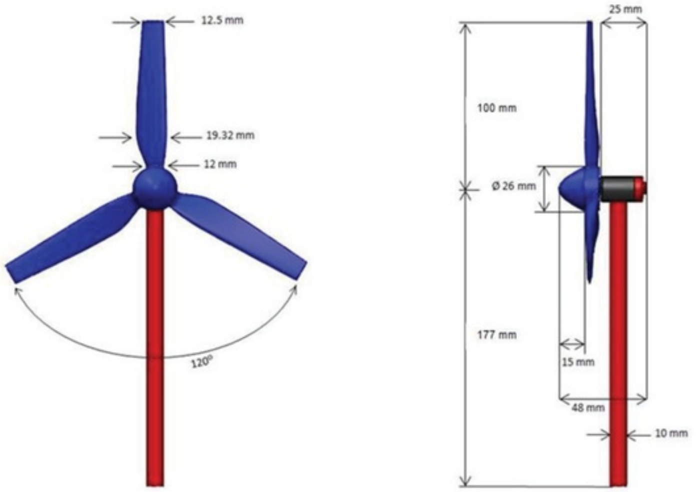

FIGURE 2. A schematic of the wind turbine model used in the present study

Wind turbine setup in the section test is shown in Figure 3. The wind velocity in test section wind tunnel was measured by a digital hot-wire anemometer (AM-4204, range 0.2-20.0 m/s) and recorded by a data acquisition system. The power generated by the wind turbine was a signal converter to direct current (GL 220, in the range 1 to 5 V) and recorded by a data acquisition system.

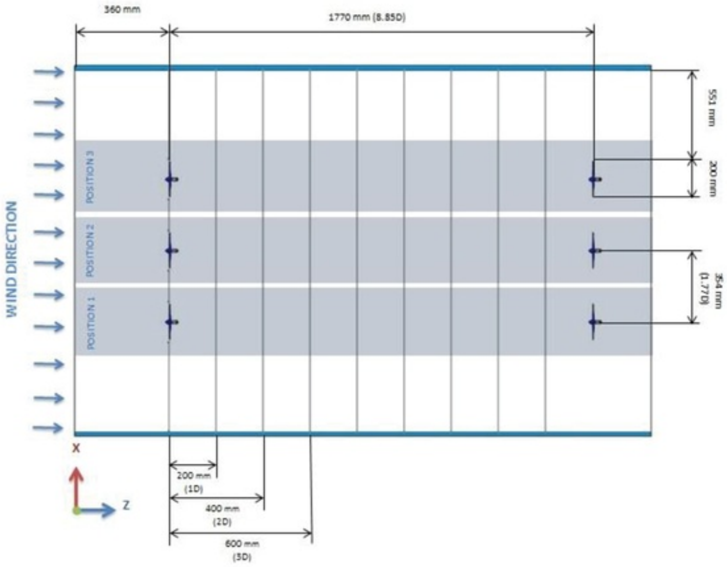

(a)

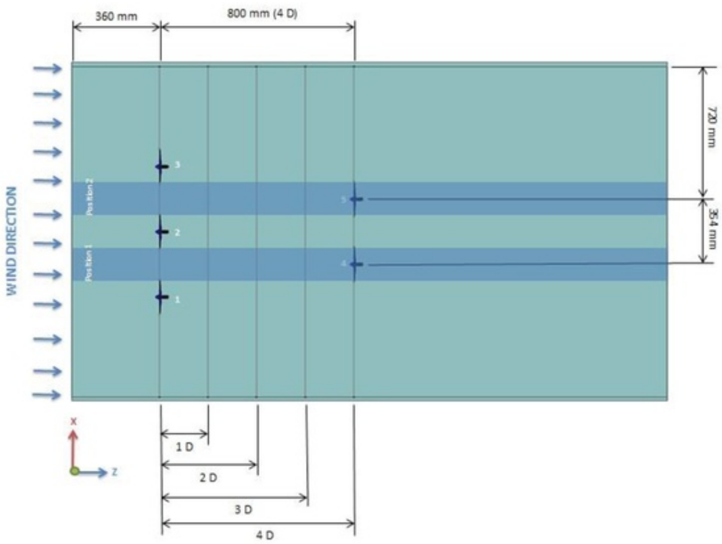

(b)

FIGURE 3. Schematic wind turbine setup in the section test, (a) Non-staggered position and (b) staggered position

Wind turbine arrays consist of 2 rows with 3 columns for spacing wind turbines in rows apart in the windward direction 1.77 rotor diameters and apart in the crosswind direction 8.85 rotor diameters. The distance between the centerline of the turbine to the side wall of the test section was kept at least 0.551 m (=2.75D) to avoid the sidewall interference. Positions 1, 2, and 3 is the location of the measurement is done either in a position staggered and non-staggered, this position is shown in Figure 3.

RESULTS AND DISCUSSION

The results of the experiment is used to discuss and compare the influence of wake flow and power production to the non-staggered and staggered position. The undisturbed wind velocity U_0 = 6.1 m/s, 0.2 m in front of the wind turbine. Lateral profiles of time averaged velocity to a non-staggered position at downwind distance z = 1D up to 8D at position 1, 2, and 3 as shown in Figure 4.

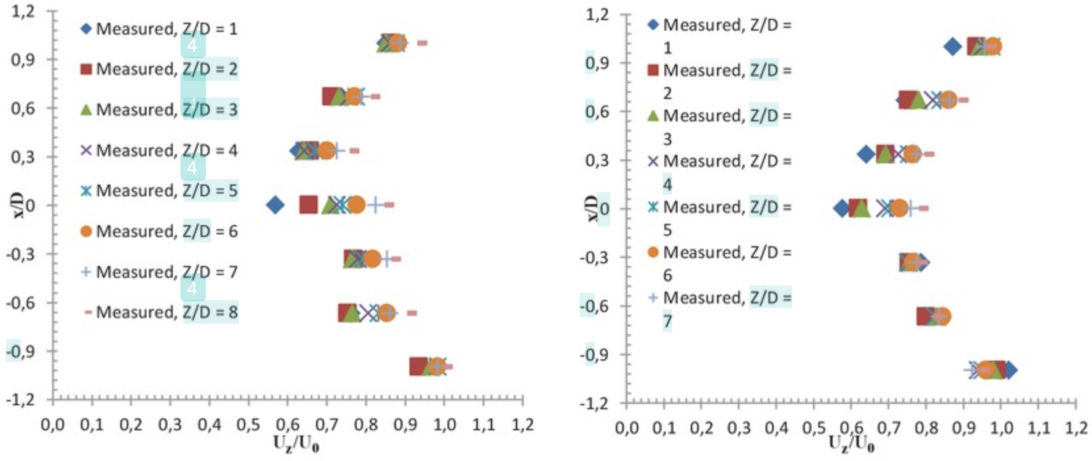

(a)

(b)

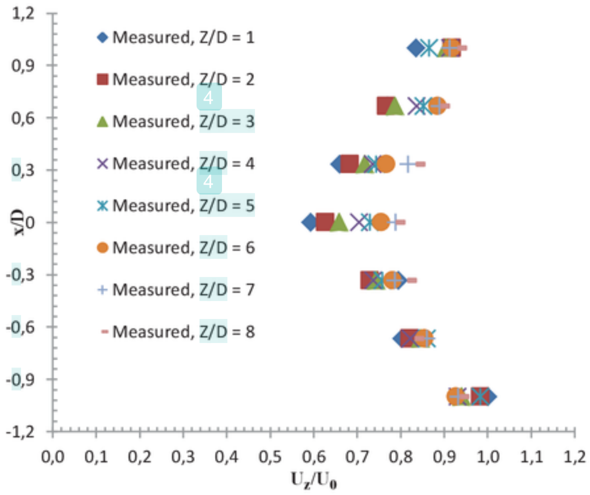

(c)

FIGURE 4. Lateral profiles of time averaged velocity to a non-staggered position at a downwind distance z = 1D up to 8D. (a) Position 1 (b) position 2 and (c) position 3

The graph measurements on lateral profiles of time averaged velocity to a non-staggered position at downwind distances z = 1D up to 8D, showed a deficit of time averaged velocity the greatest in the centre of the rotor. This is due to the air flow in the centre of the rotor restrained by the rotor hub and nacelle. The measurement results at the tip of the rotor to generate at least a small deficit of time average velocity and to measure the distance 8D of time averaged velocity to almost the same time come near to wind speed at the time of the wind turbine upwind. Lateral profile trends of time averaged velocity in the positive direction x is relatively almost the same within the negative direction x. Lateral profiles of time averaged velocity to staggered position at downwind distance z = 1D up to 3D at position 1 and 2 as shown in Figure 5.

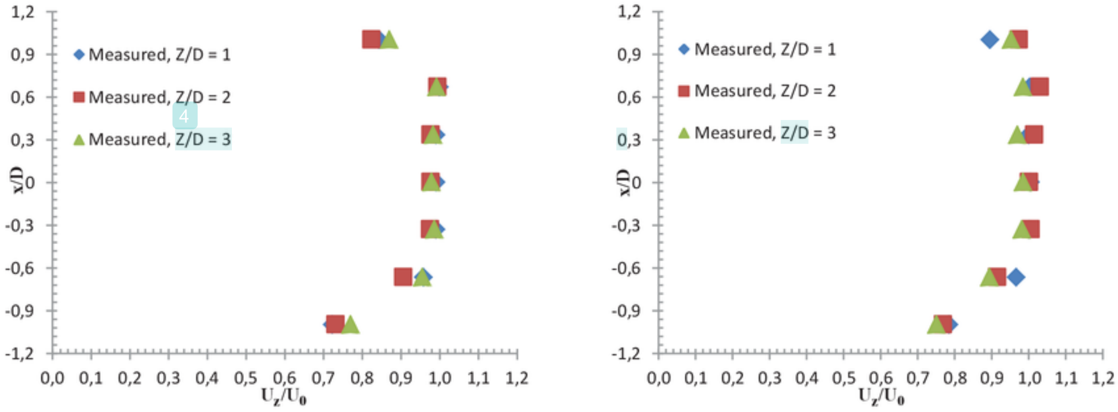

(a) (b)

FIGURE 5. Lateral profiles of time averaged velocity to staggered position at downwind distance z = 1D up to 3D. (a) Position 1 and (b) position 2

The graph measurements on lateral profiles of time averaged velocity to staggered position at downwind distances z = 1D up to 3D, showed a deficit of time averaged velocity the greatest in the tip of the rotor of the wind turbine upwind. This is due to the air flow generated by wind turbine upwind colliding at the tip of the rotor of wind turbine downwind. The results of measurements show that the centre of the rotor does not deficit the time averaged velocity both downwind distances 1D, 2D and 3D, time-averaged velocity generated the same with wind speed at the time of the wind turbine upwind. Lateral profile trends of time averaged velocity in the positive direction x is relatively almost the same within the negative direction x. The evolutions of velocity deficit at the centre line U_{c0} to a non-staggered position at position 1, 2 and 3 are shown in Figure 6 (a). The evolutions of velocity deficit at the *tip line* U_{t0} to stagger at position 1 and 2 are shown in Figure 6 (b).

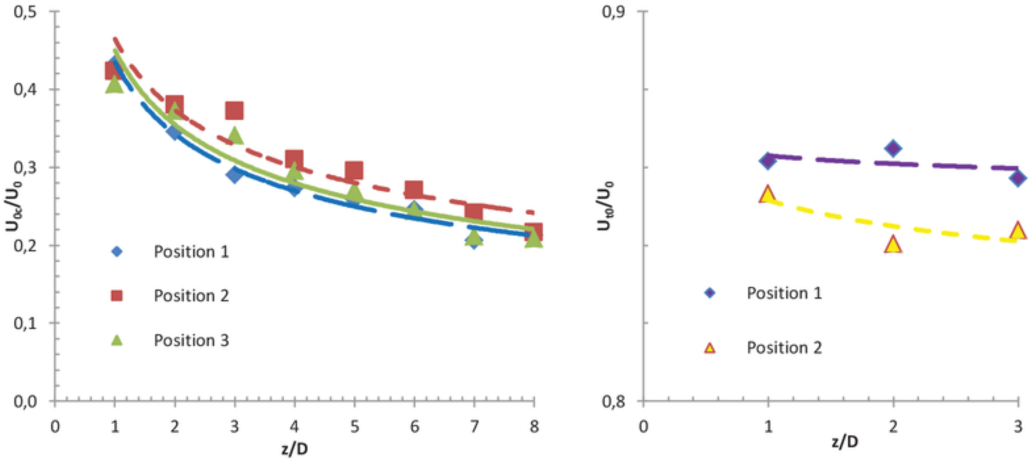

(a) (b)

FIGURE 6. (a) Centreline velocity deficit to non-staggered as a function of downwind distances. The symbols are the measured data; the lines are the predictions at position 1, 2 and 3 of Equation (2), (3) and (4), respectively. (b) Tipline velocity deficit to staggered position as a function of downwind distances. The symbols are the measured data; the lines are the predictions at position 1 and 2 of Equation (5) and (6).

The values of U_{c0} decay nonlinearly as the downwind distance increases. The relationship between the centreline velocity deficit U_{c0} and the downwind distance z at position 1 can be found by using regression analysis:

$$\frac{U_{co}}{U_o} = 0.47\left(\frac{z}{D}\right)^{-0.46} \tag{2}$$

In position 2, the centerline velocity deficit follows:

$$\frac{U_{co}}{U_o} = 0.46\left(\frac{z}{D}\right)^{-0.31} \tag{3}$$

In position 3, the centerline velocity deficit follows:

$$\frac{U_{co}}{U_o} = 0.45\left(\frac{z}{D}\right)^{-0.34} \tag{4}$$

Notice that the indices n = 0.46, 0.31 and 0.34 are smaller than the values suggested by Vermeer *et al* [14]. This is because Equations (2), (3) and (4) such as the case with Larsen *et al* [20], where a turbulent wake that is diffusing with zero ambient turbulence.

The values of U_{t0} decay nonlinearly as the downwind distance increases. The relationship between the tip line velocity deficit U_{t0} and the downwind distance z at position 1 can be found by using regression analysis:

$$\frac{U_{to}}{U_0} = 0.86\left(\frac{z}{D}\right)^{-0.003} \tag{5}$$

In position 2, the tip line velocity deficit follows:

$$\frac{U_{to}}{U_0} = 0.85\left(\frac{z}{D}\right)^{-0.01} \tag{6}$$

Notice that the indices n = 0.003 and 0.01 are smaller than the values suggested by Vermeer *et al* [14]. This is because Equations (5) and (6) such as the case with Larsen *et al* [20], where a turbulent wake that is diffusing with zero ambient turbulence.

Chu and Ching [15] defined the wake radius b as the distance from the centerline to the location where the velocity $u(r) = 0.99U_0$. The wake radius as a function of downwind distances to non-staggered position showed Figure 7 (a) at position 1, 2 and 3. The wake radius as a function of downwind distances to staggered position showed Figure 7 (b) at position 1 and 2.

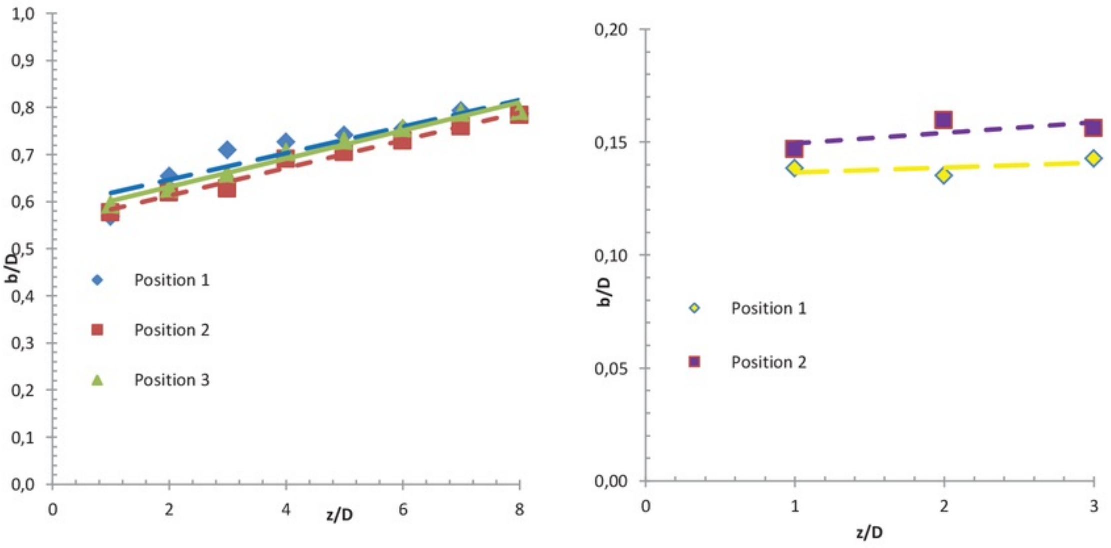

(a) (b)

FIGURE 7. (a) Wake radius as a function of downwind distances to the non-staggered position. The symbols are measured results, and the lines are the predictions at Position 1, 2 and 3 of Equation (7), (8) and (9), respectively. (b) Wake radius as a function of downwind distances to staggered position. The symbols are measured results, and the lines are the predictions at Position 1, 2 and 3 of Equation (10) and (11), respectively.

An empirical equation for the wake radius as a function of downwind distances to non-staggered position in position 1 can be found:

$$\frac{b}{D} = 0.04\left(\frac{z}{D}\right) + 0.57 \tag{7}$$

In Position 2, the wake radius is:

$$\frac{b}{D} = 0.03\left(\frac{z}{D}\right) + 0.55 \tag{8}$$

In Position 3, the wake radius is:

$$\frac{b}{D} = 0.03\left(\frac{z}{D}\right) + 0.57 \tag{9}$$

An empirical equation for the wake radius as a function of downwind distances to staggered position in position 1 can be found:

$$\frac{b}{D} = 0.002\left(\frac{z}{D}\right) + 0.13 \tag{10}$$

In Position 2, the wake radius is:

$$\frac{b}{D} = 0.005\left(\frac{z}{D}\right) + 0.15 \tag{11}$$

Results from stagger position and non-staggered position showed a significant difference. This is shown in a staggered position in the lateral direction of the rotor tip at downwind turbine is a large deficit, while in the non-staggered position opposite in the lateral direction at the centre of the turbine rotor downwind big deficit in velocity. The results shown in Figure 8 is the power generated by the turbines both non-staggered and staggered position.

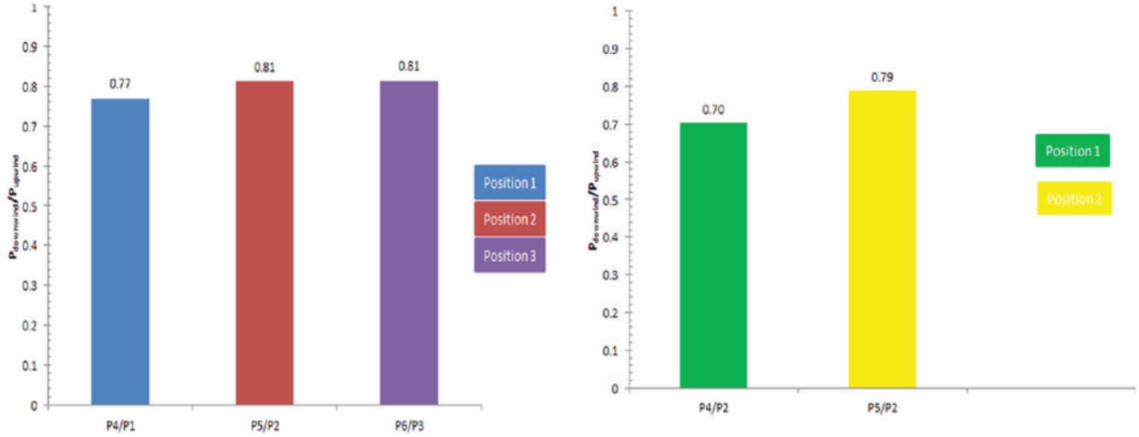

(a) (b)

FIGURE 8. (a) Compare power generated by turbine each position (non-staggered) (b) Compare power generated by turbine each position (staggered).

In this study, the power loss is due to the velocity deficit caused by the upwind turbine (non-staggered position), and six of horizontal axis wind turbines were installed in the test section {see Figure 3(a)}. The power production of the upwind turbine was measured at wind speed U_0 = 6.1 m/s. The results are shown in Figure 8 (a), as can be seen, the generated power of downwind turbine is less than the upwind turbine. The value to non-staggered position of $P_4/P_1 = 0.77$ at position 1, $P_5/P_2 = 0.81$ at position 2, and $P_6/P_3 = 0.81$ at position 3. The power loss is due to the velocity deficit caused by the upwind turbine (staggered position), and five of horizontal axis wind turbines were installed in the test section {see Figure 3(b)}. The power production of the upwind turbine was measured at wind speed U_0 = 6.1 m/s. The results are shown in Figure 8 (b), as can be seen, the generated power of downwind turbine is less than the upwind turbine. The value to staggered position of $P4/P_2 = 0.70$ and $P_5/P_2 = 0.78$.

The non-staggered position results are larger power generated than that of the staggered position, this influenced by the trend deficit in velocity that makes wind turbine generated power difference between staggered position and non-stagger position. The area used in the non-staggered position is larger than the staggered position. Resulting in the use of staggered position as one of the solutions to harness wind farms confined areas.

CONCLUSIONS

This investigation was conducted to identify the influences of the two positions (non-staggered and staggered) of wind turbine arrays. The wake characteristics such as profiles of time-averaged velocity, centerline and tip line velocity deficit, tipline velocity deficit and wake radius to the non-staggered and staggered position were measured and analysed. Based on the results of the experiment, empirical relations for the centreline velocity deficit, tipline velocity deficit and wake radius are proposed. The value to non-staggered position of $P_4/P_1 = 0.77$ at position 1, $P_5/P_2 = 0.81$ at position 2, and $P_6/P_3 = 0.81$ at position 3. The value to staggered position of $P4/P_2 = 0.70$ and $P_5/P_2 = 0.78$.The non-staggered position results are larger in power generated than that of the staggered position, this influenced by the trend deficit in velocity that makes wind turbine generated power difference between staggered position and non-stagger position. The area used non-staggered position is larger than staggered position. Resulting in the use of staggered position as one of the solutions to harness wind farms confined areas.

ACKNOWLEDGMENT

The authors gratefully acknowledge the assistance of Sulaiman Tampubolon, Azhim Asyratul azmi, Firman Ariyanto, Muhammad Leon Habibi and friends during the experiment.

REFERENCES

1. G. G. Katul, C. Angelini, D. De Canditiis, U. Amato, B. Vidakovic, and J. D. Albertson, "Are the effects of large scale flow conditions really lost through the turbulent cascade?," Geophys. Res. Lett. 30(4), 1164 (2003).
2. F. Wan, F. Port´e-Agel, and R. Stoll, "Evaluation of dynamic subgrid-scale models in large-eddy simulations of neutral turbulent flow over a two-dimensional sinusoidal hill," Atmos. Environ. 41, 2719–2728 (2007).
3. L. P. Chamorro and F. Port´e-Agel, "A wind-tunnel investigation of wind-turbine wakes: Boundary-layer turbulence effects,"Boundary-Layer Meteorol. 132(1), 129–149 (2009).
4. M. Calaf, C. Meneveau, and J. Meyers, "Large Eddy simulation study of fully developed wind-turbine array boundary layers," Phys. Fluids 22, 015110 (2010).
5. A. Singh, F. Port´e-Agel, and E. Foufoula-Georgiou, "On the influence of gravel bed dynamics on velocity power spectra,"Water Resour. Res. 46, W04509 (2010).
6. F. Wan and F. Port´e-Agel, "A large-Eddy simulation study of turbulent flow over multi scale topography," Boundary-Layer Meteorol. 141(2), 201–217 (2011).
7. L. P. Chamorro, M. Guala, R. E. A. Arndt, and F. Sotiropoulos, "On the evolution of turbulent scales in the wake of a wind turbine model," J. Turbul. 13, N27 (2012).
8. A. Singh, E. Foufoula-Georgiou, F. Port´e-Agel, and P. R. Wilcock, "Coupled dynamics of the co-evolution of bed topography, flow turbulence and sediment transport in an experimental flume," J. Geophys. Res. 117, F04016 (2012).
9. W. Zhang, C. M. Markfort, and F. Port´e-Agel, "Near-wake flow structure downwind of a wind turbine in a turbulent boundary layer," Exp. Fluids 52, 1219–1235 (2012).
10. C. J. Keylock, A. Singh, and E. Foufoula-Georgiou, "The influence of migrating bed forms on the velocity-intermittency structure of turbulent flow over a gravel bed," Geophys. Res. Lett. 40, 1351–1355 (2013).
11. A. Singh, K. B. Howard, and M. Guala, "On the homogenization of turbulent flow structures in the wake of a model wind turbine,"Phys. Fluids 26, 025103 (2014).
12. M. Magnusson and A. S. Smedman, "Air flow behind wind turbines," J.Wind Eng. Ind. Aerodyn.80,169–189 (1999).
13. K. Thomsen and P. Sorensen, "Fatigue loads for wind turbine operating in wakes," J. Wind Eng. Ind. Aerodyn.80, 121–136 (1999).
14. L. J. Vermeer, J. N. Sorensen, and A. Crespo, "Wind turbine wake aerodynamics," A., Prog. Aerosp. Sci. 39, 467-510 (2003).
15. C. R. Chu, and P. H. Ching, "Turbulence effects on the wake flow and power production of a horizontal-axis wind turbine," J. Wind Eng. Ind. Aerodyn. 124, 82-89 (2014).

16. U. Hogstrom, D. N. Asimakopoulus, H. Kambezidis, C. G. Helmis and A. Smedman, "A field study of the wake behind a 2 MW wind turbine," Atmos. Environ. 22 (4), 803-820 (1988).
17. A. Crespo and J. Hernandez, "Turbulence characteristics in wind turbine wakes," Wind Eng. Ind. Aerodyn. 61, 71-85 (1996).
18. J. Whale, K. H. Papadopaolos, C. G. Anderson, C. G. Helmis and D. J. Skyner, "A study of the near wake structure of a wind turbin comparing measurements from laboratory and full-scale experiments," Solar Energy 56 (6), 621-633 (1996).
19. Ismail, S. Kamal, Purnomo, Sarjiya, and Prajitno, "Optimized of wind farm configuration: a case study," Asian J. Applied Sciences 02 (6), 936-945 (2014).
20. G. C. Larsen, J. H^jstrup, H. A. Madsen, "Wind fields in wakes," In: Zervos A, Ehmann H, Helm P, editors. Proceedings of the 1996 European Union Wind Energy Conference, Goteborg, Sweden. p. 764–8 (1996).

Investigating the Influences of Two Position (Non-Staggered and Staggered) of Wind Turbine Arrays to produce power in a Wind Farm

ORIGINALITY REPORT

30%	12%	24%	8%
SIMILARITY INDEX	INTERNET SOURCES	PUBLICATIONS	STUDENT PAPERS

PRIMARY SOURCES

1	Chia-Ren Chu, Pei-Hung Chiang. "Turbulence effects on the wake flow and power production of a horizontal-axis wind turbine", Journal of Wind Engineering and Industrial Aerodynamics, 2014 Publication	16%
2	Submitted to Birla Institute of Technology and Science Pilani Student Paper	5%
3	www.aere.iastate.edu Internet Source	2%
4	Milanovic, Ivana M., and Khaled J. Hammad. "PIV Study of the Near-Field Region of a Turbulent Round Jet", ASME 2010 3rd Joint US-European Fluids Engineering Summer Meeting Volume 1 Symposia – Parts A B and C, 2010. Publication	2%

5	Dinaryanto, Okto, Yosephus Ardean Kurnianto Prayitno, Akmal Irfan Majid, Akhmad Zidni Hudaya, Yusnanda Agus Nusirwan, Adhika Widyaparaga, Indarto, and Deendarlianto. "Experimental investigation on the initiation and flow development of gas-liquid slug two-phase flow in a horizontal pipe", Experimental Thermal and Fluid Science, 2017. Publication	1%
6	Submitted to Universitas Diponegoro Student Paper	1%
7	Arvind Singh, Kevin B. Howard, Michele Guala. "On the homogenization of turbulent flow structures in the wake of a model wind turbine", Physics of Fluids, 2014 Publication	1%
8	www.public.iastate.edu Internet Source	1%
9	Wind Turbines, 2013. Publication	1%

Exclude quotes	Off	Exclude matches	< 1%
Exclude bibliography	On		

Investigating the Influences of Two Position (Non-Staggered and Staggered) of Wind Turbine Arrays to produce power in a Wind Farm

GRADEMARK REPORT

FINAL GRADE

/0

GENERAL COMMENTS

Instructor

PAGE 1

PAGE 2

PAGE 3

PAGE 4

PAGE 5

PAGE 6

PAGE 7

PAGE 8

PAGE 9

PAGE 10